Cation–oxygen interaction and oxygen stability in $CaCu_3Ti_4O_{12}$ and $CdCu_3Ti_4O_{12}$ lattices

2006 J. Phys.: Condens. Matter 18 1793

(http://iopscience.iop.org/0953-8984/18/5/030)

INSTITUTE OF PHYSICS PUBLISHING JOURNAL OF PHYSICS: CONDENSED MATTER

J. Phys.: Condens. Matter **18** (2006) 1793–1803 doi:10.1088/0953-8984/18/5/030

Cation–oxygen interaction and oxygen stability in $CaCu_3Ti_4O_{12}$ and $CdCu_3Ti_4O_{12}$ lattices

M Matos[1] **and L Walmsley**[2]

[1] Departamento de Física, PUC-Rio, Gávea, CEP 22453-970, Caixa Postal 38071, Rio de Janeiro, RJ, Brazil
[2] Departamento de Física, Instituto de Geociências e Ciências Exatas, Universidade Estadual Paulista, CP 178, CEP 13500-970, Rio Claro, SP, Brazil

Received 17 November 2005, in final form 19 December 2005
Published 20 January 2006
Online at stacks.iop.org/JPhysCM/18/1793

Abstract

The cubic perovskite related material $CaCu_3Ti_4O_{12}$ has attracted a great deal of attention due to the high values of the static dielectric constant, of order 10^4, approximately constant in the temperature range 100–600 K. The substitution of Ca by Cd results in a similar temperature dependence but a static dielectric constant more than one order of magnitude lower. A theoretical electronic structure study is performed on $CaCu_3Ti_4O_{12}$ (CCTO) and $CdCu_3Ti_4O_{12}$ (CdCTO) using a tight binding with overlap method. Although the calculations are performed in a paramagnetic configuration, excellent agreement with experiment was found for the calculated band gap of CCTO. In spite of the fact that the band structures of both systems look practically the same, a significant difference is found in the calculated bond strength of Ca–O and Cd–O pairs, driven by the presence of Ti, with Ca–O interaction in CCTO loosened with respect to Cd–O interaction in the cadmium compound. It is suggested that O vacancies are more easily formed in CCTO, this being related to the lower electronegativity of Ca as compared to Cd. The formation of oxygen vacancies could be the origin of the difference in the static dielectric constant of the two compounds.

1. Introduction

Scientific interest in the complex perovskite material $CaCu_3Ti_4O_{12}$ (CCTO) has grown in the last few years in view of its remarkable dielectric response [1]. CCTO presents an anomalously large static dielectric constant, reaching nearly 10^4 at room temperature and remaining constant in a large temperature range (100–600 K). CCTO is structurally similar to the more common perovskite, $CaTiO_3$. In CCTO, however, the TiO_6 octahedra are tilted to form CuO_4 (see figure 1). It is a cubic centrosymmetric crystal and no structural phase transition has yet been found [2] which could explain the high values of the static dielectric constant. Moreover, in the

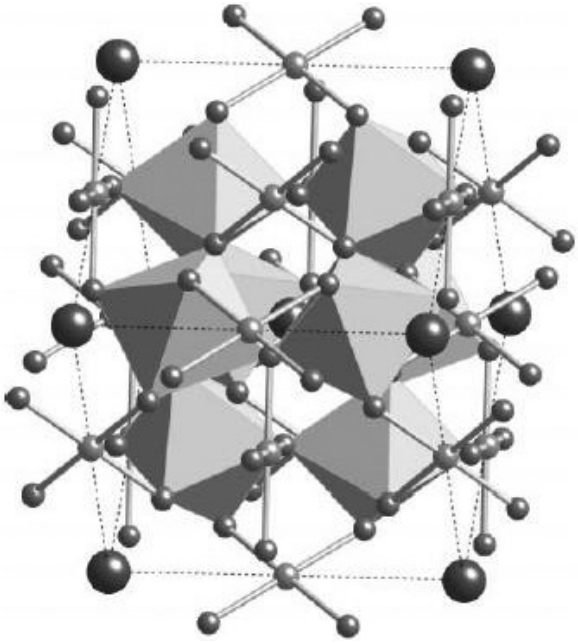

Figure 1. Crystal structure of CCTO showing Ca (bigger spheres) at the corners and centre of a cube. The squared CuO_4 sub-units (small spheres) occupy the centre of each edge of the cube. The tilted octahedra contain Ti atoms in their centre.

isostructural compound $CdCu_3Ti_4O_{12}$ (CdCTO) the static dielectric constant is more than one order of magnitude lower than in CCTO.

Structure and electronic studies have been performed on CCTO [3] using the density functional theory. Although a good agreement was found in the calculated phonon frequencies as compared with experimental data, the calculated value for the optical gap was one order of magnitude lower than the value measured experimentally. Extension to include $CdCu_3Ti_4O_{12}$ [4] has shown no significantly altered results. The static dielectric constant was also evaluated from the calculated phonon frequencies and dynamical charges in order to estimate the lattice contribution to that quantity, but only values below 100 were obtained ($\sim$40, for CCTO and $\sim$60 for CdCTO). The main conclusion of these studies is that a mechanism that would be simply related to the pure (defect-free), perfectly stoichiometric single crystal should be ruled out as being responsible for the high dielectric constant of both materials. Density functional calculations have also been performed to explain x-ray measurements in CCTO [5]. Good agreement was obtained for oxygen states even though the theoretical treatment of Cu states did not reproduce the experimental data. In particular, the band gap of CCTO was significantly underestimated. More recently, an *ab initio* study based on a spin-polarized total energy density functional theory was performed for CCTO under pressure, from zero up to 10 GPa [6]. The authors have found that, at zero temperature, between 3 and 4 GPa the material undergoes a structural transition from cubic to rhombohedral symmetry. A semiconductor–metal transition was also identified at 7 GPa. The calculated electronic structure at zero pressure was in good agreement with the results found by He *et al* [3], with a calculated indirect gap of 0.81 eV.

Without finding a good explanation in the structure, many researches started looking for extrinsic effects to explain the high dielectric constant [7] of these materials. The extrinsic

explanation would rely on the existence of charged layers, leading to the well known internal barrier layer capacitance (IBLC) mechanism, found in other high dielectric constant materials. Evidence of twin boundary layers, a frontier between two crystal regions with different TiO_6 octahedral orientation, was indeed found in CCTO [2]. However, no clear evidence has been given until recently that such layers are directly connected with the high static dielectric constant values of CCTO. Within the intrinsic mechanism, the same authors suggest that a small concentration of O vacancies could disrupt the bracing in the CCTO structure, giving rise to high dielectric constant. In this case, however, it is not clear why substitution of Ca with Cd drastically reduces the dielectric constant in all temperature ranges [1].

More recently, an impedance spectroscopy study on thin films of CCTO showed that compensation of oxygen vacancies in a post-annealing oxygen-rich atmosphere leads to an increase in the resistivity of grains and grain boundaries [8]. The authors found more evidences for the barrier layer capacitance and point out that changes in the electric properties could affect the material's dielectric properties. In another study [9], CCTO thin films with high dielectric constants were successfully grown on $Pt/Ti/SiO_2/Si(100)$ substrates. Larger dielectric relaxation, both for the dielectric constant and loss tangent, was observed when the sample was post-annealed at 550 °C in N_2 atmosphere. This effect was attributed to the generation of oxygen vacancies. After annealing the sample in an oxygen atmosphere at high temperature, which leads to oxygen vacancies compensation, the dielectric relaxation disappeared. The influence of oxygen vacancies in the dielectric properties of other transition metal oxides has already been discussed by Bosman and van Daal [10]. In reduced α-Fe_2O_3 the dielectric relaxation observed at 4.2 K is attributed to oxygen vacancies.

The possibility that the high dielectric constant of CCTO might be somewhat connected to oxygen vacancies should be considered, as an increasing number of experiments seem to point in this direction. Moreover, as was suggested by He *et al* [3], the high dielectric constant could be thought of as a combination of electronic mechanisms associated to some defects and the presence of boundary layers in the sample. In this paper we investigate the electronic structure of CCTO and CdCTO by explicitly considering the effects of oxygen interactions. The aim is to establish new insight into the role of oxygen in both materials. We use the extended Hückel theory in the calculation of the band structure, atom-resolved density of states (DOS) and inter-atomic region projected density of states, to develop atomistic models of the electronic structure of both compounds. Our main results are: (1) the calculated optical gap, of 2.81 eV, for CCTO, is in excellent agreement with experiment; in CdCTO, the gap amounts to 3.03 eV; (2) although the band structures and densities of states in CCTO and CdCTO are quite similar, a result which was also found with density functional theory calculations [4], there is a striking difference between Ca–O and Cd–O interactions; the bond strength was found to be higher, and to be *bonding* in CdCTO, a clear indication that O vacancies are more easily formed in CCTO (where Ca–O bond strengths are *anti-bonding*; (3) the relative cation–O bond strength in both materials is related to the presence of Ti, which weakens the Ca–O interaction by taking off electrons from the pair, this being related to the electronegativities of the cations.

2. Theory

Electronic structure calculations of $CaCu_3Ti_4O_{12}$ and $CdCu_3Ti_4O_{12}$ were done by using the extended Hückel approach [11, 12], a tight binding with overlap method. The method is widely known in the literature, therefore we limit ourselves to a brief explanation of some aspects which are relevant to the present discussion. Within this theoretical approach, the use of non-orthogonal basis functions allows projection of non-diagonal (inter-atomic region projected) density of states, the so-called crystal orbital overlap population (COOP) curves. COOP

analysis provides a convenient way to investigate atom-pair interactions as the integration of appropriately chosen COOP curves, throughout the occupied states (total COOP), gives quantitative estimates of bond strengths. We chose a paramagnetic state, which is described through a simple procedure of occupying band states consistently with the high spin state of Cu ions.

The tight binding parameters (see the appendix) were obtained from standard tables [13], with small modifications in Ti parameters to improve the description of the highest energy 4s and 4p bands [14]. To obtain density of states (DOS) and COOP curves, a Monkhorst–Pack [15] 14 k-point mesh was considered well suited. When several k-point sets for the reciprocal of both the primitive and the cubic crystal cells were mutually compared, we found that the calculated atomic charges agreed within 0.001. Unit cell atomic positions were taken from diffraction data of CCTO [1] and CdCTO [16]. Mulliken atomic charges are given by the integration of atom projected DOS curves.

3. Results

The crystal structure of $CaCu_3Ti_4O_{12}$ could be understood in the framework of a bcc lattice formed by Ca. The primitive bcc cell contains one formula unit. Cu occupies every edge and face of the bcc lattice, forming with Ca simple cubes whose vertices are filled in the proportion 3/4 and 1/4, respectively, for Cu and Ca. Ti atoms occupy the centres of the copper–calcium cubes. The CuO_4 sub-unit is a nearly perfect square—the two O–Cu–O angles are 95.4° and 84.6° respectively—lying equally in the xy, xz and yz planes. This small distortion could be due to the relative orientation of Ti–O bonds with regard to Ca and Cu. Note that Ti occupies the centre of a cube with six Cu and two Ca atoms at the corners. The shortest inter-atomic distances in CCTO are $d_{CaO} = 2.601$ Å, $d_{TiO} = 1.961$ Å and $d_{CuO} = 1.966$ Å.

For a better understanding of the material's band structure, we analyse first the electronic structure of the molecular ions CuO_4^{-6} and TiO_6^{-8} of $CaCu_3Ti_4O_{12}$, since they form elementary sub-units for the build-up of extended crystalline properties. The geometry of each sub-unit was carved out directly from the crystalline structure. The calculated molecular levels of each molecular fragment are shown in figure 2. Given that all CuO_4 are equivalent, the xy plane fragment was chosen as an example. Note the square planar crystal field splitting of the 3d atomic orbitals in CuO_4, with the characteristic 4 below 1 separation (figure 2(a)). The upper molecular level, occupied by the unpaired electron of Cu^{2+} ($3d^9$), is the result of oxygen mixing with $3d_{xy}$, leading to strong repulsive Cu–O interaction, consistently with the lobes of the orbital pointing at O atoms (see top of figure 2(a)). A degeneracy lifting of $3d_{xz}$ and $3d_{yz}$ could be noted in the lower set (second and third levels) with stabilization of $3d_{yz}$ (the second energy level). This is due to the distortion of the square which reduces the O–Cu–O angle bisected by the x-axis. Note that the $3d_{yz}$ orbital is farther away from the oxygens since the orbital lobes present their maximum values in the yz plane, perpendicular to the x-axis. The distortion does not affect significantly the position of other levels, especially that of $3d_{xy}$, as was seen in a calculation with a perfect square centred CuO_4. Oxygen mixing with $3d_{z^2}$ and $3d_{x^2-y^2}$ gives rise respectively to the lower and upper levels of the group. The energy separation between the lower group and the upper level is 1.64 eV. As for the TiO_6 fragment, figure 2(b) presents the usual 3 below 2 octahedral field splitting, with a t_{2g}–e_g separation of 13.5 eV. Note that all 3d levels are empty in the oxidation state Ti^{4+}. A negligible distortion is manifested in the slight splitting of the t_{2g} group, barely noticeable in the energy scale of figure 2(b). Thus, the fragment could be thought of as a practically regular octahedron.

When extended structure effects are considered, the individual molecular units generate sub-lattices, Cu–O and Ti–O, whose band structures are shown in figures 3 and 4. The sub-

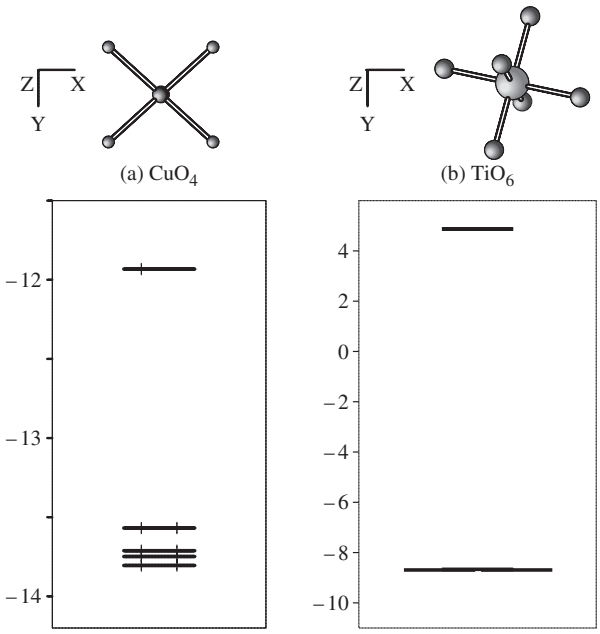

Figure 2. Molecular orbital energies (in eV) of two constituent fragments of CCTO, showing the effect of crystal field splitting of 3d atomic levels. The molecular fragments—CuO_4 and TiO_6—with (a) Cu and (b) Ti at the centre are drawn on top of each panel; note that the $3d_{xy}$ orbital of Cu is oriented towards the four O atoms. The quasi-degenerate t_{2g} and e_g orbitals of TiO_6 indicate the octahedra as almost regular. z-axis: normal to the page.

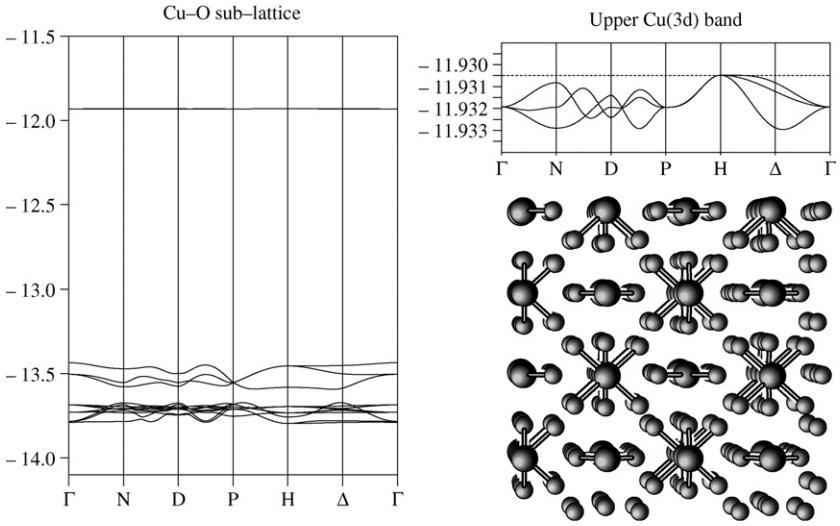

Figure 3. Band structure of the Cu–O sub-lattice of CCTO showing the Cu(3d) bands. Inset: the three $3d_{xy}$-type bands, showing the majority spin Fermi level (broken line). The sub-lattice structure is drawn from a view in the xy plane. Energies in eV.

lattice unit cell, in each case, is obtained by removing from the unit cell of CCTO the extra atoms, Ca and Ti in figure 3 and Ca and Cu in figure 4. From figure 3 it can be noted that the

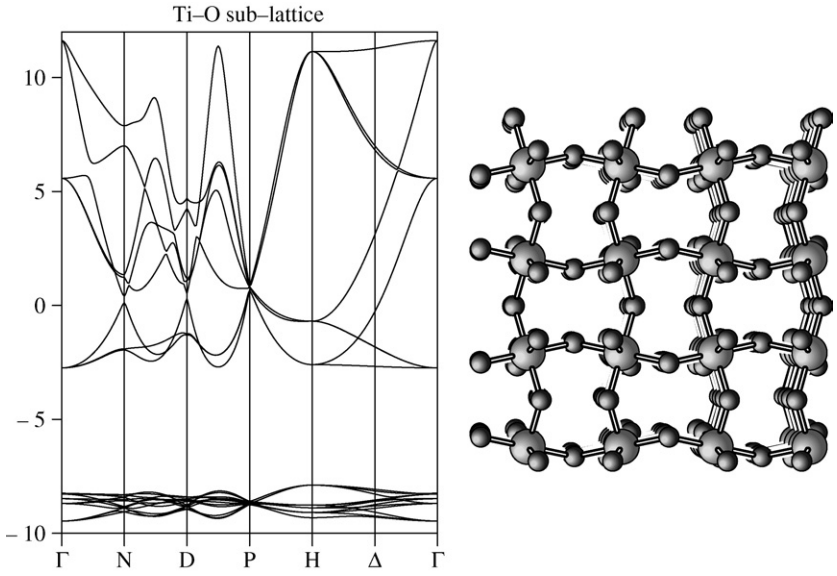

Figure 4. Band structure of the Ti–O sub-lattice of CCTO, showing the t_{2g}–e_g splitting in the extended form. The sub-lattice structure is drawn from a view in the *xy* plane, showing more clearly the tilting of TiO_6. Energies in eV.

Cu–O bands mostly reproduce the molecular level structure of the individual fragments. As the primitive unit cell contains three Cu atoms, there are $3 \times 4 = 12$ lower bands and three upper *xy*-like bands. The latter, better seen in the inset, are very narrow bands, approximately 0.002 eV-wide. At the band centre (point Γ), 1.50 eV separates the lower from the upper bands, a slightly smaller gap than the molecular value (1.64 eV), mainly due to the widening of the lower bands. The similarity between extended and molecular level structures points towards a strong localization of Cu electrons. For the Ti–O sub-lattice (figure 4), the molecular level structure is quite well reproduced in the t_{2g} bands, but strong dispersion enlarges the e_g bands (running from 2.74 to 11.6 eV). This is a common effect in tight binding with overlap calculations. It should cause no worry in the prediction of electronic properties, unless highly excited states are required, which is not the present case.

One should comment on the Fermi level position in figure 3. In the stoichiometry of the sub-lattice, $Cu_3O_{12}^{-18}$, the oxygen bands and the lower Cu bands are completely filled, but there remain three unpaired electrons to occupy the three upper Cu bands. In the usual aufbau filling scheme, two of these three electrons would occupy the lower band among the three shown in the inset of figure 3, leaving the middle band half filled. The Fermi level would then be in the middle of the upper band, not on top, as shown. In a localized picture, however, which seems more appropriate to CCTO, one should think of a paramagnetic electronic configuration in which all three bands are half filled. In figure 3 the majority spin Fermi level is represented.

The crystal structure of $CdCu_3Ti_4O_{12}$ is basically the same as that of CCTO, the only difference being the lattice parameter, approximately 1% larger [16]. Very negligible differences were obtained in the level structure of either the molecular fragments or sub-lattices of $CdCu_3Ti_4O_{12}$, when compared with those of CCTO. All considerations above therefore remain valid in the fragments and sub-lattices containing only O, Cu or Ti. This is to be expected, since these sub-systems do not contain Ca or Cd and inter-atomic distances are the same within 1%.

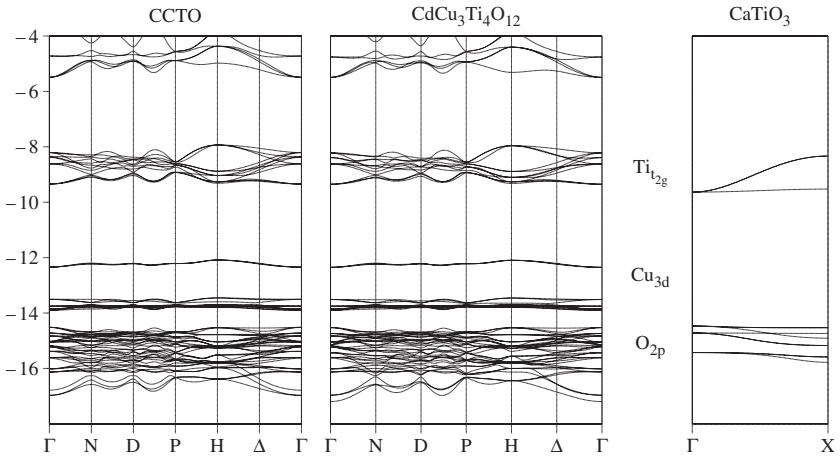

Figure 5. Band structure of CCTO, $CdCu_3Ti_4O_{12}$ and $CaTiO_3$, for comparison. Note the strong similarity in the O(2p)–Ti(t_{2g}) gap of the three compounds. The Fermi level is on top of the Cu(3d) band in the Cu containing materials (according to the text) and on top of the O(2p) band in $CaTiO_3$. Energies in eV.

We now consider the complete crystal systems of both $CaCu_3Ti_4O_{12}$ and $CdCu_3Ti_4O_{12}$, in which the influence of Ca and Cd could be noticed. However, a strong similarity was found between CCTO and CdCTO bands, a result which was already seen through density functional theory calculations [4]. The calculated band structures are shown in figure 5, which also shows calculations done for $CaTiO_3$, the more common perovskite, for comparison. Ca and Cd bands are high in energy and are not shown; the bands appearing above −6 eV come from a mixture of Ti_{e_g} with Cu_{4s} and Cu_{4p} orbitals. Note that the O, Cu and Ti bands of figure 5 are very nearly simple superpositions of the corresponding bands of the individual sub-lattices shown above, showing little hybridization. Indeed, the same point of view applies to the Cu bands in both copper containing compounds when compared with $CaTiO_3$. The Cu bands of the former enter the perovskite O–Ti gap without causing significant changes in the energy separation between the top of the O bands and the bottom of the Ti bands of CCTO and CdCTO. These results strongly confirm the localized picture suggested above for these compounds. The band states below the Fermi level are mainly a mixture of Cu_{3d} and O_{2p} orbitals, as seen from the analysis above, in agreement with previous *ab initio* calculations [3, 6].

In table 1, more data on calculated electronic properties are given. Note first that the band gap, a transition from the higher lying Cu to the lowest unoccupied $Ti_{t_{2g}}$ bands, is nearly the same in the Ca (2.81 eV) and Cd (3.03 eV) compounds. The CCTO value is in very good agreement with experimental estimates of the optical gap for this material, which is found to stay above 1.5 eV [7]. Furthermore, it is the presence of Cu which is responsible for the strong decrease of the optical gap in CCTO and CdCTO, as compared to the most common perovskites. The extended Hückel calculated value for $CaTiO_3$ is 4.7 eV, corresponding to a transition between O(2p) to Ti(t_{2g}) bands. The experimental value obtained for the orthorhombic structure of calcium titanate stays in the range 2.8–3.5 eV [17]. It is worth pointing out that the good experimental agreement found for the calculated band gap of CCTO is related to the use of the paramagnetic band filling scheme. This provides a correct description of the electronic structure of the material, through the presence of a gap right above the highest occupied Cu band.

Table 1. Several results of calculated electronic structure.

	CCTO	$CdCu_3Ti_4O_{12}$
Net atomic charge		
Cu	1.126	1.118
Ti	1.713	1.892
Ca/Cd	2.139	1.093
O	−1.031	−1.001
Average COOP		
Cu–O	0.204	0.187
Ti–O	0.426	0.387
Ca/Cd–O	−0.019	0.095
Cu–Ti	0.003	0.002
Ca/Cd–Ti	−0.023	0.016
Ca/Cd–Cu	−0.008	−0.008
First forbidden electronic transition (in eV)		
	2.81	3.03

More significant differences are observed in the calculated Mulliken charges of Ca (2.139) and Cd (1.093). The electron loss in Ti and O is nearly the same in both materials; the Cu charge is also hardly affected by the cation substitution. Qualitatively, our results for the calculated Mulliken charges in CCTO are very similar with previous *ab initio* calculations [6]. In both cases, a considerable amount of charge transfer from Ca, Ti and Cu to O was found, with Ti and Ca providing the largest positive charge.

A more striking effect of cation substitution can be noted in the calculated total COOP involving Ca or Cd interaction with O and Ti in the two perovskite-like materials. Note from table 1 that in $CdCu_3Ti_4O_{12}$ the total Cd–O (Cd–Ti) COOP is +0.095 (+0.016), denoting that such atom-pair interactions give a net bonding contribution to the electronic energy per unit cell. On the other hand, a net anti-bonding contribution arises in CCTO for Ca–O and Ca–Ti pairs, as seen from the negative values of the total COOP (−0.019 and −0.023, respectively). Since the total COOP gives a measure of the bond strength, these results indicate that breaking cation–O and –Ti bonds in CCTO is easier than in the Cd compound. As a consequence it could be expected that O–vacancy formation is more likely to occur in CCTO. Note that the distinction between Ca–O and Cd–O interactions, even though clearly seen in a COOP kind of analysis, causes no easily visible differences in the band structure of the materials, because the latter exposes the simultaneous effect of all interactions in the system. The rise in the bond strength for Cd pairs is consistent with the lower atomic charge of this cation as compared with Ca; both are due to a more dense electron distribution around Cd.

The weaker Ca bond strengths, as compared with Cd, are more strongly associated with Ti. This could be seen in a series of calculations performed on different model systems. For instance, in molecular coordinated clusters, CaO_{12}^{-22} and CdO_{12}^{-22}, taken directly from the crystal structures, the Ca–O and Cd–O bond strengths were found to be 0.079 and 0.121, respectively. Note the bonding nature of Ca–O interaction, in contrast to the anti-bonding one in CCTO. Quantitatively, the same results were found for these bond strengths in several Ti-lacking sub-lattices. The ones considered were Ca/Cd–O and Ca/Cd–O–Cu sub-lattices, carved out from both the CCTO and CdCTO crystals. Therefore, the strongly different behavior of Ca and Cd in the actual compounds, especially the Ca interactions turning anti-bonding, can be ascribed to

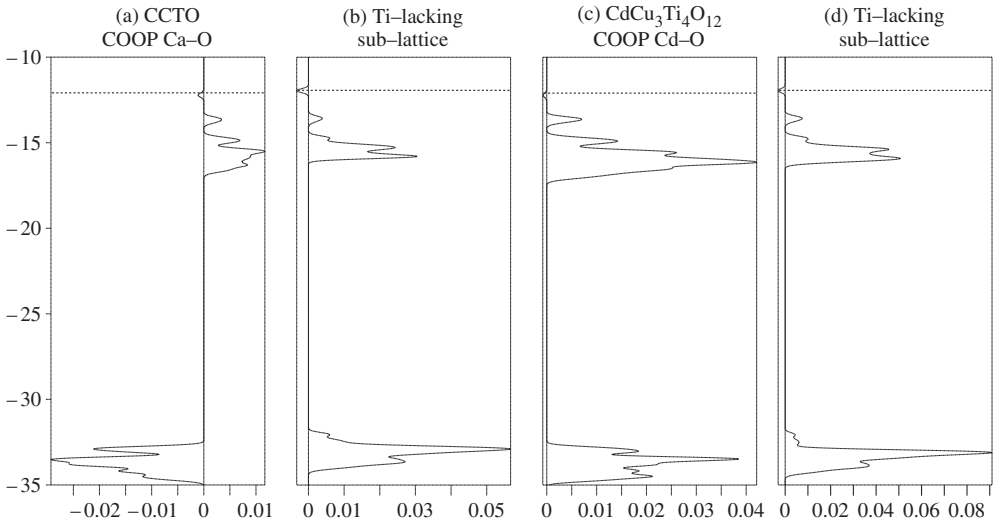

Figure 6. COOP curves for Ca–O or Cd–O interaction in (a) CCTO and (c) $CdCu_3Ti_4O_{12}$. The same atom-pair COOP curves are shown in (b) CCTO and (d) $CdCu_3Ti_4O_{12}$ sub-lattices not containing Ti. Energies are in eV. The numbers in the horizontal scale provide a measure of the COOP and could be understood as the character of the contribution of the given pair (atom or orbital) to the DOS, as a function of energy; positive (negative) COOP denotes bonding (anti-bonding) combination.

the presence of Ti in the lattices. Note also that no changes are noticed when one goes from the molecular to the extended Ca–O sub-units. To stress this idea further, a calculation was done in Cu-lacking sub-lattices of CCTO and CdCTO, that is, Ti–Ca/Cd–O sub-lattices. As one could expect, one gets −0.021 and 0.093 respectively for Ca–O and Cd–O bond strengths, different from the values obtained in the Ti-lacking sub-structures and very close to those found in both the perovskite ($Ca/CdTiO_3$) and perovskite-like materials.

The total COOPs between Cu and the other cations, Ti and Ca(Cd), are about one order of magnitude smaller than that of Cu–O, consistent with localization. The role of Cu may therefore be thought of as being mainly structural, on the one hand, favouring, through the formation of the square planar CuO_4, the tilting of TiO_6. On the other hand, Cu also modifies electrical and optical properties by reducing the forbidden gap in the perovskite-like materials, which might then be characterized as semi-conducting [8].

The pair interaction properties discussed above are well related to electron affinities, respectively 1.0 for Ca, 1.3 for Ti and 1.5 for Cd. Thus, Ti takes electrons from Ca, of lower electronegativity, being less effective in weakening Cd bonds. This weakens the several bonds of Ca in CCTO with respect to those with Cd. In terms of extended Hückel parameters, the atomic energy terms, H_{ii}, which are taken from experimental ionization energies, are consistent with this picture. Note from the appendix that Ca atomic energy levels (H_{ii}) stay above those of Cd and Ti levels.

Some COOP curves, whose integration give the bond strengths (total COOPs) discussed above, are shown in figure 6. They illustrate with more detail the effects of Cd substitution in CCTO. Note the negative Ca–O COOP in CCTO (figure 6(a)), indicating anti-bonding interaction in the O(2s) band (below −30 eV). In figure 6(b), where Ti is arbitrarily taken off from the CCTO lattice, the Ca–O COOP becomes positive. In the O_{2p} band, the absence of Ti also contributes to enhancing the Ca–O COOP, as could be noted from the COOP scale

(horizontal scale of the graphics). On the other hand, there is bonding Cd–O interaction in this energy range in both $CdCu_3Ti_4O_{12}$ (figure 6(c)) and corresponding Ti-lacking lattices (figure 6(d)), showing that Ti causes no weakening of Cd–O interaction in CdCTO. The COOP values are, in fact, smaller for CCTO in all the energy range below the Fermi level, consistent with the results shown above in the several sub-lattices and molecular clusters (leading to stronger Cd–O bond strength). Ti is extracted as a +4 ion, so that the Fermi level stays at the top of the Cu(3d) upper band.

4. Conclusion

In this work, a theoretical electronic structure study was performed in $CaCu_3Ti_4O_{12}$ and $CdCu_3Ti_4O_{12}$ by using the extended Hückel method within a paramagnetic electronic configuration. The calculations show strong similarity in the band structure of both systems. Since the compounds have the same structure, with the difference in lattice parameters of only 1%, this should not be surprising. However, a striking effect of cation substitution was noted in the calculated total COOP involving Ca or Cd interaction with O and Ti in the two perovskite-like materials, this being related to the relationship between the electronegativities of Ca, Cd and Ti. Taking into account that the total COOP gives a measure of the bond strength, the present results indicate that breaking cation–O and –Ti bonds in CCTO is easier than in the Cd compound. As a consequence, it could be expected that O–vacancy formation is more likely to occur in CCTO. Oxygen vacancies are important in explaining the high dielectric constant in CCTO. The fact that O atoms are more tightly bound in CdCTO could then be a clue to understanding why the dielectric constant in CdCTO is lower than in CCTO.

The extended Hückel method was shown to provide a good insight into basic electronic mechanisms of these complex compounds. In particular, with the use of a paramagnetic band filling scheme, excellent agreement is found between the calculated and experimental band gap of CCTO. The role of Cu was found to be both structural, by allowing TiO_6 octahedral tilting, and electrical, by reducing the optical gap with respect to the more common $CaTiO_3$ perovskite.

Acknowledgments

All calculations in this paper were done with the *yaehmop* package, developed by Dr Greg Lundrum.

Appendix

For each atom in the unit cell, there are two atomic parameters to be specified for the build-up of the extended Hückel Hamiltonian, namely, H_{ii}, the atomic energy term and ζ_i, the Slater atomic orbital exponent. In this paper, we have used the following parameters: (a) for O, $H_{2s,2s} = -32.3$ eV with $\zeta_{2s} = 2.275$, $H_{2p,2p} = -14.8$ eV with $\zeta_{2p} = 2.275$; (b) for Ca, $H_{4s,4s} = -7.0$ eV with $\zeta_{4s} = 1.2$, $H_{4p,4p} = -4.0$ eV with $\zeta_{4p} = 1.2$; (c) for Cu, $H_{4s,4s} = -11.4$ eV with $\zeta_{4s} = 2.2$, $H_{4p,4p} = -6.06$ eV with $\zeta_{4p} = 2.2$, $H_{3d,3d} = -14.0$ eV with $\zeta_1 = 5.95$ and $\zeta_2 = 2.30$ in a linear double zeta combination with coefficients $c_1 = 0.5933$ and $c_2 = 0.5744$, respectively and (d) for Ti, $H_{4s,4s} = -8.97$ eV with $\zeta_{4s} = 1.075$, $H_{4p,4p} = -5.44$ eV with $\zeta_{4p} = 1.075$, $H_{3d,3d} = -10.81$ eV with $\zeta_1 = 4.55$ and $\zeta_2 = 1.40$ in a linear double zeta combination with coefficients $c_1 = 0.4206$ and $c_2 = 0.7839$, respectively.

References

[1] Subramanian M A, Li D, Duan N, Reisner B A and Sleight A W 2000 *J. Solid State Chem.* **151** 323–5
[2] Subramanian M A and Sleight A W 2002 *J. Solid State Sci.* **4** 347–51
[3] He L, Neaton J B, Cohen M H, Vanderblit D and Homes C C 2002 *Phys. Rev.* B **65** 214112
[4] He L, Neaton J B, Vanderblit D and Cohen M H 2003 *Phys. Rev.* B **67** 012103
[5] McGuiness C, Downes J E, Sheridan P, Glans P-A, Smith K E, Si W and Johnson P D 2005 *Phys. Rev.* B **71** 195111
[6] Fagan S B, Souza Filho A G, Ayala A O and Filho J M 2005 *Phys. Rev.* B **72** 014106
[7] Homes C C, Vogt T, Shapiro S M, Wakimoto S, Subramanian M A and Ramirez A P 2003 *Phys. Rev.* B **67** 092106
[8] Fang L, Shen M, Li Z and Cao W 2004 *Preprint* cond-mat/0408275
[9] Fang L, Shen M and Cao W 2004 *J. Appl. Phys.* **95** 6483
[10] Bosman A J and van Daal H J 1970 *Adv. Phys.* **19** 1
[11] Hoffmann R 1963 *J. Chem. Phys.* **39** 1397–412
Whangbo M-H and Hoffmann R 1978 *J. Am. Chem. Soc.* **100** 6093–8
[12] Hoffmann R 1988 *Solids and Surfaces* (New York: VCH)
[13] *Tables of Parameters for Extended Hückel Calculations* 1993 Collected by Santiago Alvarez, Universitat de Barcelona
[14] Matos M, Hoffmann R, Latgé A and Anda E V 1996 *Chem. Mater.* **8** 2324–30
[15] Monkhorst H J and Pack J D 1976 *Phys. Rev.* B **13** 5188
Mehl M J, Osburn J E, Papaconstantopoulos D A and Klein B M 1990 *Phys. Rev.* B **41** 10311
[16] Deschanvres A, Raveau B and Tollemer F 1967 *Bull. Soc. Chim. Fr.* **11** 4077
[17] Bak T, Nowotny J, Sorrel C C, Zhou M F and Vance E R 2004 *J. Mater. Sci. Mater. Electron.* **15** 635–44